Full Articles

Specific spectral properties of a photochromic ferromagnetic $(C_{25}H_{23}N_3O_3Cl)CrMn(C_2O_4)_3 \cdot H_2O$

S. M. Aldoshin,[a] N. A. Sanina,[a]★ V. A. Nadtochenko,[a] E. A. Yur´eva,[a] V. I. Minkin,[b] N. A. Voloshin,[b] V. N. Ikorskii,[c]† and V. I. Ovcharenko[c]

[a]*Institute of Problems of Chemical Physics, Russian Academy of Sciences, 1 prosp. Akad. Semenova, 142432 Chernogolovka, Moscow Region, Russian Federation. Fax: +7 (496) 524 9676. E-mail: sanina@icp.ac.ru*
[b]*Southern Scientific Center of the Russian Academy of Sciences, 41 prosp. Chekhova, 344006 Rostov-on-Don, Russian Federation*
[c]*International Tomography Center, Siberian Branch of the Russian Academy of Sciences, 3a ul. Institutskaya, 630090 Novosibirsk, Russian Federation*

A molecular magnetic $(C_{25}H_{23}N_3O_3Cl)CrMn(C_2O_4)_3 \cdot H_2O$ whose spiropyran cation contains a quaternized pyridine fragment in the side aliphatic chain was synthesized for the first time. The compound possesses the properties of a ferromagnetic with T_c = 5.2 K and photochromic properties in the crystalline state. The photochemical properties of the hybrid compound were studied by electronic and IR spectroscopies. Photochromic transformations of the spiropyran cation are accompanied by the appearance of a broad absorption band in the region 400—600 nm in the electronic spectra and by reduction of intensity of the $\nu(C_{spiro}—O)$ IR band at 942 cm^{-1}.

Key words: molecular magnetics, (tris)oxalates, polyfunctional compounds, photochromism, spiropyrans.

Recently, researchers have paid attention to combinatorial design of hybrid polyfunctional materials promising for practical applications in molecular electronics. This makes it possible to fabricate crystalline materials that combine "building blocks" responsible for different physicochemical properties, *e.g.*, photochromism and magnetism,[1—4] photochromism and conduction,[5—8] electrical and magnetic properties,[9—11] and optical dichroism and magnetism[12,13] in the same lattice. When studying the mutual effects of the building blocks, modifying the properties of particular blocks, and imparting novel functions to hybrid materials (synergistic effect), research on the properties of the functional components of the materials is of particular importance. Analysis of specific features of

† Deceased.

Published in Russian in *Izvestiya Akademii Nauk. Seriya Khimicheskaya,* No. 6, pp. 1055—1061, June, 2007.

the molecular and crystal structure of various photochromic crystalline spiropyran salts[14,15] revealed some regularities responsible for reversible photochromic transformations of the cationic sublattice of spiropyran in the crystal. They can be useful for the synthesis of novel hybrid photochromic magnetics. Earlier,[4] we established that the photochromic properties of the hybrid polycrystals are reversible and that the stability of the colored form in these crystals increases by several orders of magnitude compared to solutions.

In this work we synthesized polycrystals of a new hybrid compound based on 1-{(5′-chloro-1′,3′,3′-trimethyl-6-nitrospiro[2*H*-1-benzopyran-2,2′-indolin]-8-yl)methyl}pyridinium chloride (**1**) containing a quaternized pyridine moiety in the side aliphatic chain and the magnetic anion $[CrMn(C_2O_4)_3]^-$. We also studied the spectral and magnetic properties of compound **1**.

Experimental

^{1}H NMR spectra were recorded on a Varian Unity-300 spectrometer (300 MHz) with Me_4Si as internal reference; the chemical shifts (δ) and spin-spin coupling constants (*J*) were determined to an accuracy of 0.01 ppm and 0.1 Hz, respectively. 5-Chloro-1,3,3-trimethyl-2-methylideneindoline (**2**) was purchased from Aldrich. Compound **3** was synthesized following a known procedure.[4] Elemental analysis was performed at the Analytical Center (Institute of Problems of Chemical Physics, Russian Academy of Sciences).

1-{(5′-Chloro-1′,3′,3′-trimethyl-6-nitrospiro[2*H*-1-benzopyran-2,2′-indolyn]-8-yl)methyl}pyridinium chloride (1). A solution of compound **2** (0.42 g, 2 mmol) in MeOH (2 mL) was added to a boiling mixture of aldehyde **3** (0.59 g, 2 mmol) and MeOH (14 mL) over a period of 30 min. The mixture was refluxed for 4 h, the solvent was evaporated, and the residue was recrystallized from acetonitrile. Yield 0.55 g (57%). Found (%): C, 62.10; H, 4.96; N, 8.53. $C_{25}H_{23}Cl_2N_3O_3$. Calculated (%): C, 61.99; H, 4.79; N, 8.67. ^{1}H NMR ($CDCl_3$), δ: 0.83, 1.11 (both s, 3 H each, C(3′)H_3); 2.61 (s, 3 H, C(1′)H_3); 5.82 (d, 1 H, H(3), *J* = 10.4 Hz); 6.08, 6.30 (both d, 1 H, C(8)$\underline{H}_2$Py, *J* = 14.1 Hz); 6.54 (d, 1 H, H(7′), *J* = 8.3 Hz); 6.90 (d, 1 H, H(4′), *J* = 2.1 Hz); 6.95 (d, 1 H, H(4), *J* = 10.4 Hz); 7.26 (dd, 1 H, H(6′), *J* = 8.2 Hz, *J* = 2.1 Hz); 7.72 (dd, 2 H, $H(3)_{Py}$, $H(5)_{Py}$, *J* = 7.8 Hz, *J* = 6.7 Hz); 8.04 (d, 1 H, H(5), *J* = 2.6 Hz); 8.37 (tt, 1 H, $H(4)_{Py}$, *J* = 7.8 Hz, *J* = 1.1 Hz); 8.87—8.90 (m, 3 H, $H(2)_{Py}$, $H(6)_{Py}$, H(7)).

Complex $(C_{25}H_{23}N_3O_3Cl)CrMn(C_2O_4)_3\cdot H_2O$ (4) was synthesized following the known procedure.[4] Yield 25%.* Found (%): C, 44.15; H, 3.05; Cr, 6.24; Mn, 6.52; N, 4.98. $C_{31}H_{25}ClCrMnN_3O_{16}$. Calculated (%): C, 44.42; H, 2.99; Cr, 6.21; Mn, 6.56; N, 5.02.

Magnetic measurements. The magnetic susceptibility of complex **4** was measured using a Quantum Design SQUID magnetometer in the temperature range 2—300 K in magnetic fields of strength up to 10 kOe. The effective magnetic moment was calculated from the equation

$$\mu_{eff} = [(3k/N\beta^2)\chi T]^{0.5} \approx (8\chi T)^{0.5},$$

where χ is the molar paramagnetic susceptibility, *k* is the Boltzmann constant, *N* is the Avogadro constant, and β is the Bohr magneton.

Photochemical studies. Electronic absorption spectra of compound **4** were recorded on a Perkin—Elmer Lambda EZ 210 spectrometer using fine-crystalline powder samples dispersed in Nujol mull (layer ~2 μm thick). The mass fraction of powder was about 70%. IR Fourier spectra were recorded on a Perkin—Elmer Spectrum BX II spectrometer with a spectral resolution of 4 cm^{-1} (64 scan accumulation). Samples were prepared in the form of KBr pellets (180 mg of KBr and ~1 mg of compounds **1** or **4**). During all measurements, samples were placed at the same positions in the instruments to exclude variations of the base line depending on the powder scattering at different position relative to the optical axis of the instrument.

Samples were irradiated with UV light of a PL-S 9W gas-discharge low-pressure mercury lamp whose inner wall was coated with a luminophore emitting in the UV (340—400 nm) region with a maximum at 355 nm. Irradiation with visible light was carried out using a light-emitting diode (λ = 530 nm, power 60 mW, light spot diameter 1.5 cm).

Experimental data were processed using the Igor Pro 4.0 program. The background spectra were subtracted from the IR spectra under study.

Results and Discussion

Spiropyran **1** was synthesized by the reaction of methylideneindoline **2** with pyridinium methyl-substituted aldehyde **3** following a known procedure[4] (Scheme 1).*

Scheme 1

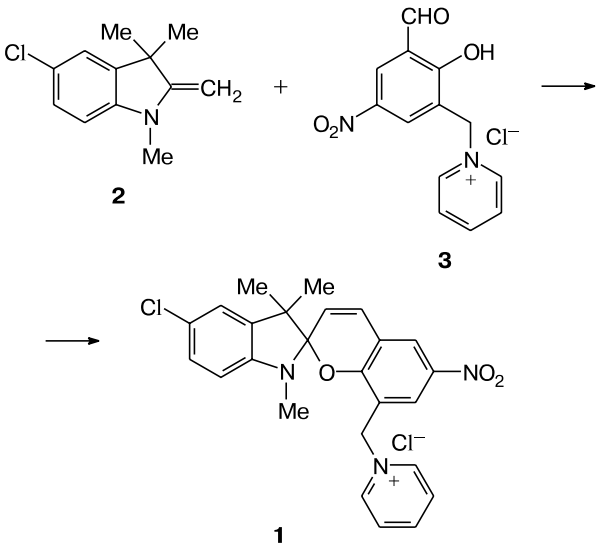

* A ferromagnetic containing a H atom in position 5′ of the indoline fragment of the cation was obtained[4] in much higher yield.

* Cationic spiropyrans of the type **1** can also be synthesized by the reaction of pyridine with 6-nitro-8-chloromethylspirobenzopyranindoline.[16,17]

Polycrystals of the bimetallic hybrid complex were synthesized following the published procedure[4] (Scheme 2).

Scheme 2

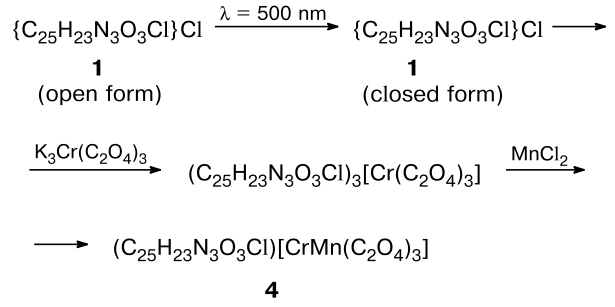

Magnetic properties. Complex **4** exhibits the properties of a ferromagnetic with a Curie temperature of 5.2 K (determined from the magnetization measurements in a weak magnetic field). The magnetization of the sample is plotted *vs.* magnetic field strength at 2 K in Fig. 1. At $H =$ 10000 Oe, the magnetization is almost saturation, being equal to 6.87 μ_B. This is somewhat lower than the value of 8 μ_B expected for the eight-spin (3 + 5 = 8) $Cr^{III}Mn^{II}$ configuration. The coercive force is about 36 Oe (half the hysteresis loop, see plot shown in Fig. 1).

The effective magnetic moment (μ_{eff}) at 300 K is 6.91 μ_B, being in good agreement with the value calculated for weakly interacting Mn^{II} and Cr^{III} ions, namely, 7.07 μ_B ($g = 2$). As the temperature decreases, the μ_{eff} value increases due to the ferromagnetic exchange interactions in complex **4**. The magnetic susceptibility at $T > 10$ K obeys the Curie—Weiss law

$$\chi = C/(T - \theta)$$

with the parameters $C = 5.77$ cm^3 K mol^{-1} and $\theta = 7.7$ K. The positive value of the Weiss constant θ is also an indication of ferromagnetic interactions in the complex. The parameter $1/\chi$ is plotted *vs.* $(T - 7.7)/5.77$ in Fig. 2 (solid line).

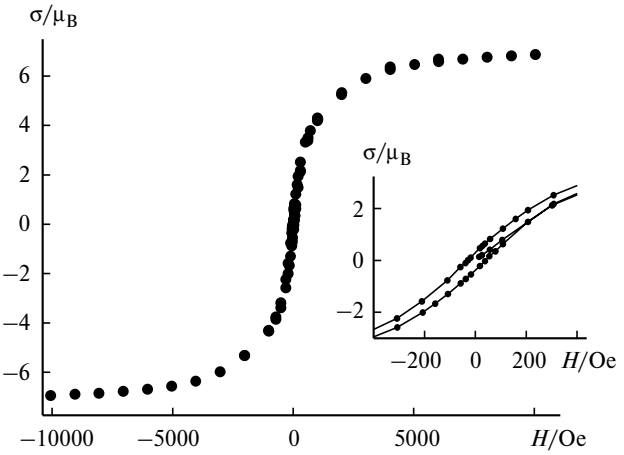

Fig. 1. Magnetization (σ) of complex **4** plotted *vs.* magnetic field strength (H) at 2 K. The inset shows a portion of the curve in weak fields.

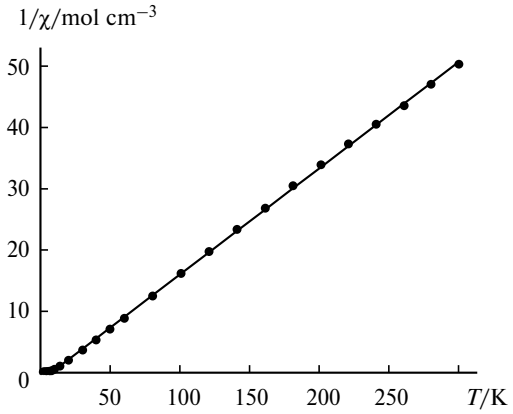

Fig. 2. Inverse magnetic susceptibility ($1/\chi$) of complex **4** plotted *vs.* temperature.

Photochemical properties. The photochromic properties of compound **4** are characteristic of spiropyrans. The mechanism of the photochromic transformation involves conversion between the open and closed forms (denoted by "*O*" and "*C*", respectively) under irradiation with UV and visible light (Scheme 3). In the dark, both forms are observed. The rate of equilibration under these conditions is negligible compared to the rates of the processes occurring under irradiation, which are discussed below. There-

Scheme 3

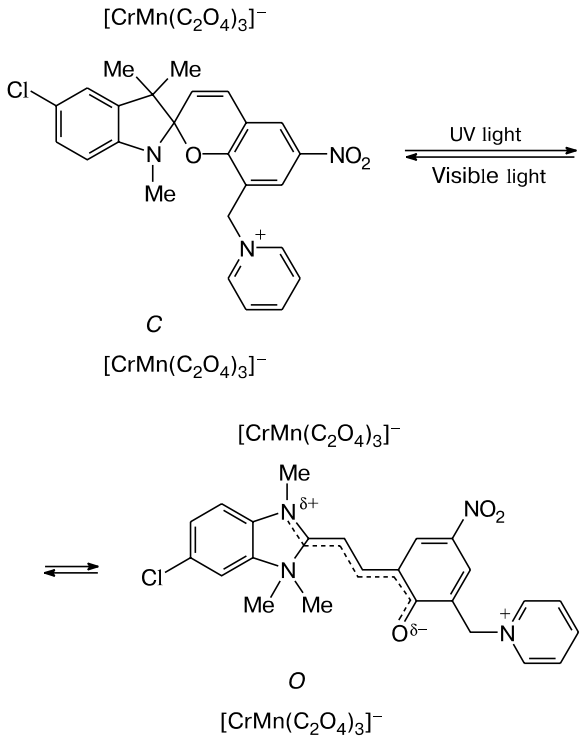

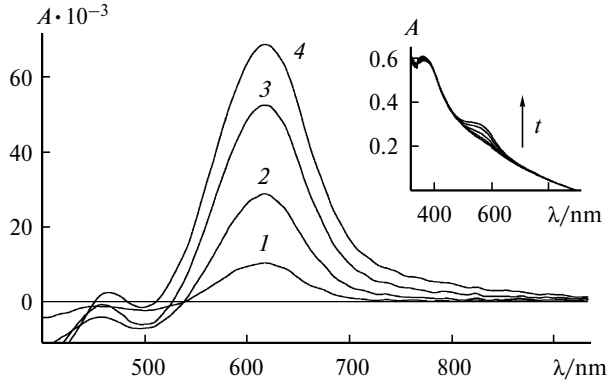

Fig. 3. Changes in the difference electronic absorption spectra of polycrystals **4** with time upon UV irradiation: t = 0.5 (*1*), 2 (*2*), 10 (*3*), and 50 min (*4*). The inset shows the changes in the electronic absorption spectra polycrystals **4** with time upon UV irradiation.

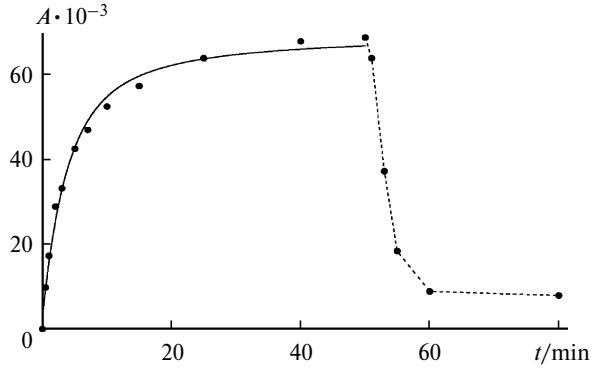

Fig. 5. Kinetics of changes in the absorption of polycrystals **4** at λ = 567 nm during irradiation with UV (0—50 min) and visible (50—80 min) light: points denote experimental data, the solid line passing to t = 50 min represents the results of approximation by the function $D(t) = c_1\{1 - [1/(c_2t)](1 - e^{-c2t})\}$, where c_1 = 0.073(1) and c_2 = 0.34(3).

fore, the dark reactions are left out of consideration in this work.

Change in the absorption spectra of complex **4** upon irradiation at λ = 355 nm are shown in the inset in Fig. 3. UV irradiation of the sample causes the appearance of a spectral band in the region 500—650 nm, which corresponds to the formation of the open form. The difference spectra of complex **4** (see Fig. 3) were obtained by subtracting the spectrum of the non-irradiated sample from that of the irradiated sample. The longer the UV irradiation, the more intense the broad band with a maximum at about 567 nm.

Exposure of the sample to visible light causes disappearance of the absorption of the open form at 567 nm (Fig. 4) and bleaching of the sample. The spectrum does not return to its initial pattern (this is clearly seen in the kinetic curve shown in Fig. 5), namely, it exhibits residual absorption in the region 400—600 nm even after the first irradiation cycle (UV irradiation for 50 min followed by exposure to visible light for 30 min). As the number of irradiation cycles increases, the intensity of this broad band rapidly increases (Fig. 6); thus, the area under the spectral curve in the region of the maximum corresponding to the open form decreases.

The equilibration kinetics observed under UV irradiation at λ = 355 nm is shown in Fig. 5. The kinetic curve does not obey an exponential law. This can be explained by either nonuniform light intensity distribution $I(x,t)$ within crystals or nonuniform distribution of reaction centers due to nonuniform local molecular environment.

Consider the first case. Since light penetrates the material to a distance of about 0.5 μm,[18] while the size of a polycrystal is at most 5 μm, the light intensity distribution

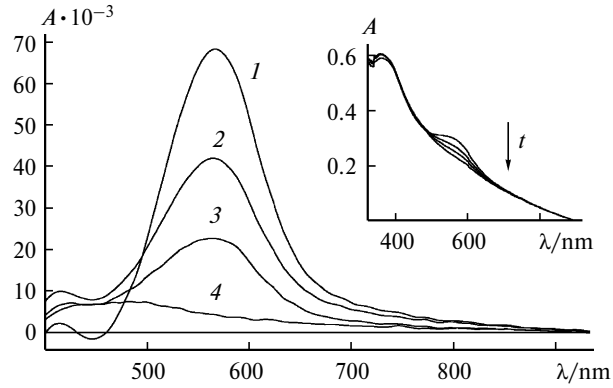

Fig. 4. Changes in the difference electronic absorption spectra of polycrystals **4** with time upon irradiation with visible light: t = 0 (*1*), 1 (*2*), 3 (*3*), and 30 min (*4*). The inset shows the changes in the electronic absorption spectra of polycrystals **4** with time upon exposure to visible light.

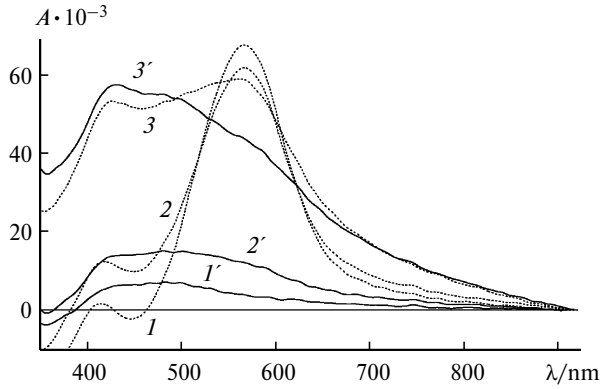

Fig. 6. Changes in the difference electronic absorption spectra of polycrystals **4** after the first (*1*, *1′*), second (*2*, *2′*), and fifth (*3*, *3′*) cycles of irradiation at λ = 355 (*1—3*) and 530 nm (*1′—3′*).

$I(x,t)$ in the crystal is *a priori* nonuniform. The equilibration kinetics obeys the law

$$d[O(x,t)]/dt = \{-[\varepsilon_O(\lambda)\varphi_O(\lambda) + \varepsilon_C(\lambda)\varphi_C(\lambda)] \cdot [O] + \varepsilon_C(\lambda)\varphi_C(\lambda)A\} \cdot I(x,t), \quad (1)$$

where $\varepsilon_O(\lambda)$ and $\varepsilon_C(\lambda)$ are the extinction coefficients of the "*O*" and "*C*" forms, respectively; $\varphi_O(\lambda)$ and $\varphi_C(\lambda)$ are the quantum yields of formation of the "*O*" and "*C*" forms, respectively; $[O]$ is the equilibrium concentration of the open form; $A = [O] + [C] = \text{const}$; and $I(x,t)$ is the light intensity distribution within crystals.

Equation (1) can be integrated by simplifying the expression for $I(x,t)$ and approximating $I(x) = I_0 \cdot e^{-ax}$

$$[O](t) = 1/\alpha\{1 - [1/(I_0\sigma t)](1 - e^{-I_0\sigma t})\}, \quad (2)$$

where α is the light absorption coefficient; $\sigma = \varepsilon_O\varphi_O + \varepsilon_C\varphi_C$; ε_O and ε_C are respectively the extinction coefficients of the open and closed forms at the excitation wavelength; φ_O and φ_C are the quantum yields of the photochemical reaction of the spiropyran ring opening and closure, respectively; and I_0 is the intensity of incident light.

Figure 5 shows that function (2) satisfactorily describes the experimental data using two variable parameters, α and σ.

We believe that nonexponential kinetics are a consequence of nonuniform distribution of light passing through the sample. However, significant inhomogeneity of the local molecular environment can manifest itself in polycrystals; therefore, one can assume that the contour of the open-form absorption band changes in the course of the reaction. We will analyze changes in the band half-width as a characteristic of the bandshape. The absorption band contour is described by a Gaussian line (see inset in Fig. 7). At 17768±11 cm^{-1}, the band half-width changes by 700 cm^{-1}. Therefore, the spectral maximum retains its position within the limits of measuring error. This suggests that irradiation causes a gradual, increasingly deeper, layer-by-layer penetration of light into the material and formation of new reaction centers responsible for inhomogeneous line broadening. The lack of isosbestic point can be explained by analogy, namely, assuming that several nonequilibrium processes occur in the system at different rates.

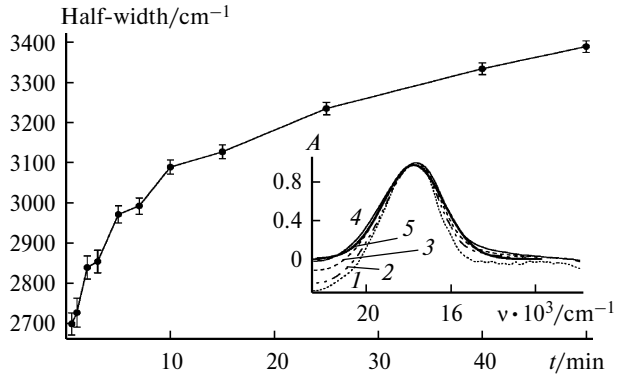

Fig. 7. Changes in half-width maximum absorption of complex **4** at $\lambda = 567$ nm with time upon UV irradiation ($\lambda = 355$ nm). The inset shows the changes in the difference absorption spectra upon UV irradiation ($\lambda = 355$ nm): $t = 0.5$ (*1*), 2 (*2*), 10 (*3*), and 50 min (*4*); and a Gaussian line (*5*). The data are normalized to the absorption at $\lambda = 567$ nm.

Photochemical transformations of the spiropyran cation in polycrystals can be studied in more detail by IR Fourier spectroscopy. The IR spectra of spiropyran **1** powder and polycrystals **4** are shown in Fig. 8 and the wavenumbers and intensities of the key vibrational bands are listed in Table 1. Band assignment for the closed form of spiropyran **1** was based on the published data.[19—21] Namely, the ν_{as}(O—H) and ν_s(O—H) stretching vibrations of bound water correspond to a broad peak in the region 3600—3300 cm^{-1}; the stretching bands of CH_2 and CH_3 groups are observed at 2931 (ν_{as}(C—H)) and 2870 cm^{-1} (ν_s(C—H)); aromatic vibrations ν(C—H) correspond to the bands at 3048, 3028, and 2988 cm^{-1}; the in-plane vibrations β(C—H) correspond to the band at 1484 cm^{-1}; the antisymmetric ($\nu_{as}(NO_2)$) and symmetric ($\nu_s(NO_2)$) vibrations are observed at 1526 and 1339 cm^{-1}, respectively; bending vibrations of aromatic rings are observed at 1607, 1587, 1460, and 1164 cm^{-1}; the out-of-plane vibrations γ(C—H) correspond to the bands at 810 and 786 cm^{-1}; and $\nu(C_{spiro}—O)$ vibrations are at 942 cm^{-1}. The band at 1423 cm^{-1} probably corresponds to the N—CH_3 vibrations in the indoline fragment of the molecule. Bending vibrations of bound water δ(H—O—H) appear near 1631 cm^{-1}.

Compared to the IR spectrum of compound **1**, that of complex **4** shows additional bands at 1707, 1667, and 1396 cm^{-1}, which can be attributed to vibrations of the oxalate network, a much more intense δ(H—O—H) band at 1631 cm^{-1}, and much weaker ν(C—H) stretching bands.

Changes in the difference IR spectra of complex **4** and spiropyran **1** in the region 1700—700 cm^{-1} upon UV irradiation ($\lambda = 355$ nm) are shown in Fig. 9. The difference spectra were obtained by subtracting the spectrum of the non-irradiated sample from the spectrum recorded after irradiation. The IR spectra significantly change throughout the whole spectral region studied, the changes being similar for complex **4** and compound **1**. In this work we consider the behavior of the $\nu_{as}(NO_2)$, $\nu_s(NO_2)$, and $\nu(C_{spiro}—O)$ absorption bands in more detail. UV-Irradiation of polycrystals **1** and **4** causes reduction of the intensities of these IR bands. The degree of conversion is 20% for complex **4** and 4% for compound **1**. The kinetics of changes in the absorption of the open form also obeys a non-exponential law.

The $\nu(C_{spiro}—O)$ band experiences the greatest changes (Fig. 10), which indicates cleavage of the C_{spiro}—O bond

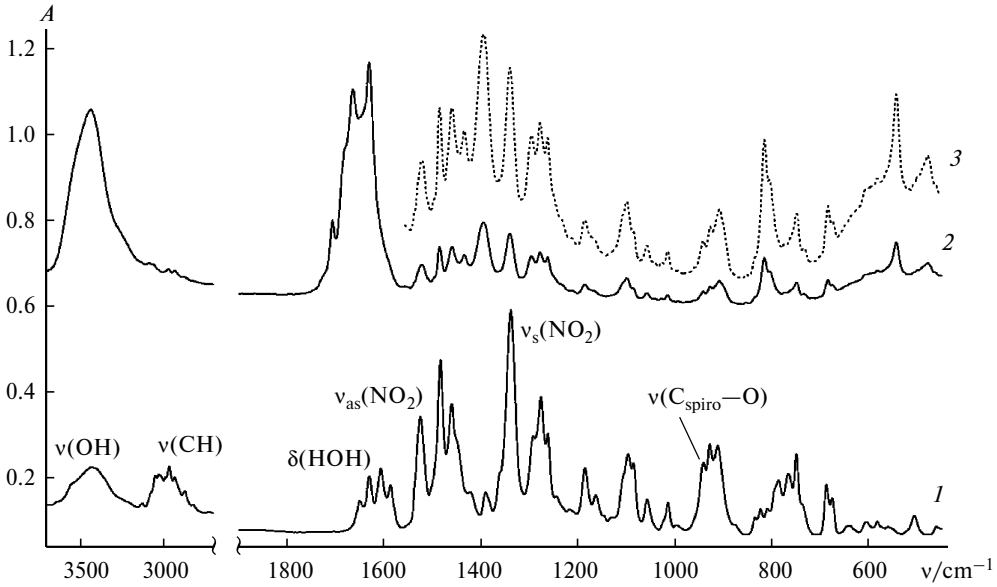

Fig. 8. IR spectra of powder spiropyran **1** (*1*) and polycrystals of complex **4** (*2*). Spectrum *2* is shifted along the ordinate axis by a value of 0.5. The fragment of the spectrum *2* in the region 1580—450 cm^{-1} (*3*) is magnified (×3).

as a result of the photochemical reaction. But because the open and closed forms have different geometries, vibrations of all bonds in the cation should be redistributed simultaneously. Therefore, in fact the IR spectra exhibit either reduction of intensity or a shift of a number of bands.

Irradiation of the samples with visible light (λ = 530 nm) causes an increase in the intensity of the $\nu_s(NO_2)$, $\nu(C_{spiro}—O)$, and some other vibrational bands. However, the band intensities do not reach their initial values, which is in good agreement with the electronic spectra of the same samples. The intensity of the $\nu_{as}(NO_2)$ band does not increase upon irradiation of polycrystals **1** and **4** with visible light; moreover, it continues to monotonically decrease. This behavior is due to higher "sensitivity" of the $\nu_{as}(NO_2)$ band to lattice distortions, which are most probably determined by differences between the geometric parameters of the open and closed forms. Irrevers-

Table 1. Wavenumbers (ν) and intensities (*I*) of key bands in the IR spectrum of compound **1**

ν/cm^{-1}	*I*	Assigned based on Refs 19—21	ν/cm^{-1}	*I*	Assigned based on Refs 19—21
3048	34	—	1245	26	—
3028	35	ν(C—H) arom.	1218	21	—
2988	34	—	1186	38	—
2965	38	ν(C—H) in CH_3	1164	27	ν(C=C)
2931	34	ν_{as}(C—H) in CH_3	1097	43	—
2870	28	ν_s(C—H) in CH_3	1086	39	—
1652	25	ν(C=C)	1058	25	—
1631	34	δ(H—O—H)	1014	24	—
1607	37	—	942	39	(C_{spiro}—O)
1587	31	ν(C=C)	928	47	—
1526	58	$\nu_{as}(NO_2)$	912	46	—
1484	80	β(C—H)	835	18	—
1460	63	ν(C=C)	824	21	—
1423	28	ν(C—N)	810	22	γ(C—H)
1391	28	δ(CH_3)	786	33	γ(C—H)
1339	100	$\nu_s(NO_2)$	766	35	—
1293	50	—	750	43	—
1277	66	(N—C—O)	688	31	—
1263	51	—	676	26	—

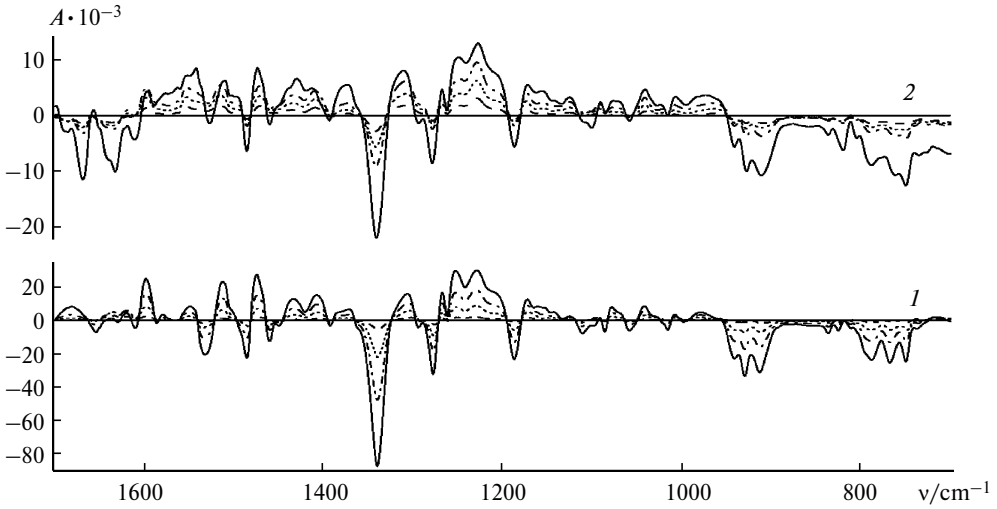

Fig. 9. Changes in the difference IR spectra of polycrystals **1** (*1*) and **4** (*2*) in the region 1700—700 cm^{-1}.

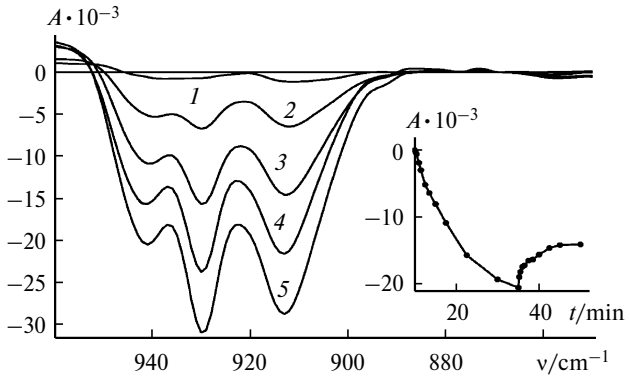

Fig. 10. Changes in the difference IR spectra compound **1** with time during UV irradiation in the region of the $\nu(C_{spiro}—O)$ band: t = 1 (*1*), 5 (*2*), 10 (*3*), 25 (*4*), and 50 min (*5*). The inset shows the kinetics of changes in the absorption at 941 cm^{-1} of the sample of compound **1** during irradiation with UV (region 0—50 min) and visible light (region 50—80 min).

ible changes in the IR spectra due to the formation of by-products will be discussed elsewhere.

Compound **4** possesses the properties of a photochromic ferromagnetic with a Curie temperature of 5.2 K. UV-Irradiation of a polycrystalline sample of complex **4** causes the appearance of the band with a maximum at 567 nm in the absorption spectra, which indicates the formation of the open form of spiropyran. The kinetics of the rise of the merocyanine absorption maximum obeys a non-exponential law. The changes observed are reversible and irradiation of the colored sample with visible light causes the absorption of the open form to disappear, but the spectrum does not return to the initial pattern; the residual absorption in the region 400—600 nm is still observed. These changes in the IR spectra of complex **4** also characterize the occurrence of a photochemical reaction. Exposure of the sample to UV light leads to a decrease in the intensity of the $\nu(C_{spiro}—O)$ band at 942 cm^{-1}, which indicates the opening of the furan ring. Exposure to visible light causes an increase in the intensity of this band; however, the IR spectrum does not return to the initial pattern. Thus, the reverse photochemical ring closure reaction does not go to completion.

This work was financially supported by the Presidium of the Russian Academy of Sciences (Basic Research Program "Target Synthesis of Compounds with Preset Properties and Design of Functional Materials Based on Them").

References

1. S. Benard, E. Riviere, and P. Yu, *Chem. Mater.*, 2001, **13**, 159.
2. S. Benard and P. Yu, *Chem. Commun.*, 2000, 65.
3. I. Kashima, M. Okubo, Y. Ono, M. Itoi, N. Kida, M. Hikita, M. Enomoto, and N. Kojima, *Synth. Met.*, 2005, **153**, 473.
4. S. M. Aldoshin, N. A. Sanina, V. I. Minkin, N. A. Voloshin, V. N. Ikorskii, V. I. Ovcharenko, V. A. Smirnov, and N. K. Nagaeva, *J. Mol. Struct.*, 2007, **826**, 69.
5. L. V. Zorina, S. S. Khasanov, R. P. Shibaeva, I. Yu. Shevyakova, A. I. Kotov, and E. B. Yagubskii, *Kristallografiya*, 2004, **49**, 1113 [*Crystallogr. Repts*, 2004, **49** (Engl. Transl.)].
6. R. Shibaeva, S. Khasanov, L. Zorina, S. Simonov, I. Shevyakova, L. Kushch, L. Buravov, E. Yagubskii, S. Boudron, C. Meziere, P. Batail, E. Canadell, and J. Yamada, *J. Phys. IV (Fr.)*, 2004, **114**, 481.
7. I. Shevyakova, L. Buravov, V. Tkacheva, L. Zorina, S. Khasanov, S. Simonov, J. Yamada, E. Canadell, R. Shibaeva, and E. Yagubskii, *Adv. Funct. Mater.*, 2004, **14**, 660.
8. S. V. Simonov, I. Yu. Shevyakova, L. V. Zorina, S. S. Khasanov, L. I. Buravov, V. A. Emel´yanov, E. Canadell, R. P. Shibaeva, and E. B. Yagubskii, *J. Mater. Chem.*, 2005, **15**, 2476.

9. T. G. Prokhorova, S. S. Khasanov, L. V. Zorina, L. I. Buravov, V. A. Tkacheva, A. A. Baskakov, R. B. Morgunov, M. Gener, E. Canadell, R. P. Shibaeva, and E. B. Yagubskii, *Adv. Funct. Mater.*, 2003, **13**, 403.
10. R. P. Shibaeva, E. B. Yagubskii, E. Canadell, S. S. Khasanov, L. V. Zorina, L. A. Kushch, T. G. Prokhorova, I. Yu. Shevyakova, L. I. Buravov, V. A. Tkacheva, and M. Gener, *Synth. Met.*, 2003, **133—134**, 373.
11. R. B. Morgunov, A. A. Baskakov, L. R. Dunin-Barkovskiy, S. S. Khasanov, R. P. Shibaeva, T. G. Prokhorova, E. B. Yagubskii, T. Kato, and Y. Tanimoto, *J. Phys. IV (Fr.)*, 2004, **114**, 335.
12. M. Gruselle, C. Train, F. Villain, N. S. Ovanesyan, V. D. Makhaev, and C. Cordier, *Mendeleev Commun.*, 2004, 284.
13. N. S. Ovanesyan, V. D. Makhaev, S. M. Aldoshin, P. Gredin, K. Boubekeur, C. Train, and M. Gruselle, *J. Chem. Soc., Dalton Trans.*, 2005, **18**, 3101.
14. S. M. Aldoshin, L. A. Nikonova, V. A. Smirnov, G. V. Shilov, and N. K. Nagaeva, *Izv. Akad. Nauk. Ser. Khim.*, 2005, 2050 [*Russ. Chem. Bull., Int. Ed.*, 2005, **54**, 2113].
15. S. M. Aldoshin, L. A. Nikonova, V. A. Smirnov, G. V. Shilov, and N. K. Nagaeva, *J. Mol. Struct.*, 2005, **750**, 158.
16. K. Takagi, T. Kurematsu, and Y. Sawaki, *J. Chem. Soc., Perkin Trans. 2*, 1995, 1667.
17. T. Noguchi, M. Kikuchi, and T. Kakurai, *Nippon Kagaku Zasshi*, 1972, 1323.
18. S. M. Aldoshin, L. A. Nikonova, G. V. Shilov, E. A. Bikanina, N. K. Artemova, and V. A. Smirnov, *J. Mol. Struct.*, 2006, **794**, 103.
19. G. Arnold and G. Paal, *Tetrahedron*, 1971, **27**, 1699.
20. G. Arnold and C. Schiele, *Tetrahedron Lett.*, 1967, **13**, 1191.
21. G. Arnold and C. Schiele, *Z. Naturforsch.*, 1967, **22b**, 1228.

Received November 21, 2006;
in revised form April 13, 2007